Published in final edited form as:
Kidney Int. 2011 September ; 80(5): 493–503. doi:10.1038/ki.2011.125.

Acute loss of renal function abolishes slow leukocyte rolling and transmigration by interfering with intracellular-signaling molecules

Jan Rossaint[1,2], **Oliver Spelten**[1,2], **Nadja Kässens**[1,2], **Helena Mueller**[1,2], **Hugo Van Aken**[1], **Kai Singbartl**[3], and **Alexander Zarbock**[1,2]

[1]Department of Anesthesiology and Intensive Care Medicine, University of Münster, Germany

[2]Max-Planck Institute of Molecular Biomedicine, Münster, Germany

[3]Department of Critical Care Medicine, University of Pittsburgh, USA

Abstract

Acute kidney injury (AKI) is a common clinical problem in critically ill patients and increases in-hospital mortality. Acute loss of renal function (ALRF) reduces leukocyte recruitment into inflamed tissue, but the underlying molecular mechanisms remain unknown. In this study, we investigated the effects of ALRF on the different steps of the leukocyte recruitment cascade by using intravital microscopy, flow chamber experiments, and biochemistry assays. ALRF abolished selectin-induced slow leukocyte rolling on E-selectin/ICAM-1 and P-selectin/ICAM-1 and also reduced transmigration without affecting chemokine-induced arrest. A reduced phosphorylation of spleen tyrosine kinase (Syk), Akt, phospholipase C (PLC) γ2, and p38 MAPK, but not altered expression levels of adhesion molecules on the surface of neutrophils, was responsible for the abolished selectin-mediated slow leukocyte rolling. The results observed in the murine system could be reproduced in flow chamber experiments with human blood. Samples from critically ill patients with sepsis-induced AKI showed a significantly higher rolling velocity on E-selectin/ICAM-1 and P-selectin/ICAM-1 compared to patients with sepsis alone or to healthy volunteers. In conclusion, these data suggest that ALRF inhibits selectin-mediated slow leukocyte rolling by reducing phosphorylation of Syk, Akt, PLCγ2, and p38 MAPK and transmigration.

Keywords

Acute kidney injury; acute loss of renal function; sepsis; leukocyte recruitment; signaling; phospholipase C γ2; p38 MAPK; spleen tyrosine kinase; Akt

Introduction

Acute kidney injury (AKI) is a common problem in critically ill patients and increases morbidity and mortality (1–5). Sepsis is the leading cause of AKI in critically ill patients (3). Patients with sepsis-induced AKI require renal replacement therapy more often and also have a higher adjusted risk for both short- and longterm mortality (2).

Corresponding author: Alexander Zarbock, M.D., University of Münster, Department of Anesthesiology and Critical Care Medicine, Albert-Schweitzer Str. 33, 48149 Münster, Germany, Phone: +49 (251) 8347252, Fax: +49 (251) 88704, zarbock@uni-muenster.de.

Disclosure

Conflict-of-interest disclosure: The authors declare no competing financial interests.

We have previously shown that acute loss of renal function (ALRF) attenuates the severity of aseptic acute lung injury by inhibiting neutrophil recruitment into the inflamed lung (6). Chronic loss of renal function caused by chronic kidney disease alters neutrophil and lymphocyte function and leads to induction of apoptosis (7–10).

Although impaired neutrophil recruitment during AKI appears to be beneficial in the setting of aseptic lung injury, these findings certainly raise concerns for the combined occurrence of AKI and bacterial infections. These concerns are further substantiated by clinical observations. For example, patients with AKI more frequently demonstrate bacteremia and poor outcome in the setting of peritonitis, hematologic malignancies, and after cardiac surgery than patients without AKI (11–14). The underlying mechanisms for these observations also remain unclear.

The classical leukocyte recruitment cascade comprises ‘capturing’ (‘tethering’), rolling, slow rolling, arrest, post-adhesion strengthening, crawling, and transmigration (15). ‘Capturing’ is the first contact between neutrophils and the endothelium of postcapillary venules and is mediated by selectins and their main counter-receptor, P-selectin glycoprotein ligand-1 (PSGL-1), on neutrophils. During this initial step, selectins and chemokines presented on the inflamed endothelium activate signaling pathways in neutrophils that regulate integrin adhesiveness. Binding of activated integrins to their counter-receptor leads, depending on the conformational state of the integrin, either to a reduction of the rolling velocity or arrest. PSGL-1 engagement induces the active, extended conformation of the β_2-integrin lymphocyte function-associated antigen-1 (LFA-1) leading to the transition from rolling to slow rolling (16). PSGL-1 engagement by E-selectin induces the phosphorylation of the Src kinase Fgr and the ITAM-containing adaptor proteins DAP12 and FcRγ which subsequently associate with Syk (17). The Tec family kinase Bruton tyrosine kinase (Btk) is downstream of Syk and regulates two pathways (18, 19). One is phospholipase (PLC) γ2- and the other phosphoinositide 3-kinase (PI3K) γ-dependent (19). p38 MAPK is located in the PLCγ2-dependent signaling pathway (19). Following selectin engagement, p38 MAPK is phosphorylated and blocking of p38 MAPK by a pharmacologic inhibitor increases the rolling velocity on E-selectin/ICAM-1 compared to the control group (16, 20).

During the interaction of leukocytes with inflamed endothelium, leukocytes are exposed to chemokines that bind to and activate chemokine receptors on neutrophils (21). The activation of these G-protein coupled receptors leads to the activation of the phospholipases C (PLC) β_2 and PLC β_3 (22, 23). PLC isoforms hydrolyze phosphatidylinositol 4,5-biphosphate to produce inositol-triphosphate (IP_3) and diacylglycerol, which mobilize Ca^{2+} from nonmitochondrial stores and induce downstream signaling (24). Chemokines fully activate integrins, which subsequently bind to their counter-receptors on endothelial cells and mediate adhesion (15).

The last step in the recruitment cascade is the transmigration, when leukocytes leave the intravascular compartment and enter the tissue. Leukocyte transendothelial cell migration can occur either directly through individual endothelial cells (transcellular route) or between endothelial junctions (paracellular route). Several endothelial membrane proteins, most of them located at endothelial cell contacts, have been shown to be involved in leukocyte diapedesis (25).

The present study was designed to investigate the effect of ALRF on the different steps of the leukocyte recruitment cascade during local or systemic inflammation. Using *ex vivo* flow chamber assays, *in vivo* inflammation experiments, and *in vitro* phosphorylation assays, we demonstrate that ALRF inhibits selectin-mediated slow leukocyte rolling by reducing phosphorylation of Syk, Akt, PLCγ2. and p38 MAPK and transmigration.

Results

ALRF leads to inhibition of P-selectin mediated neutrophil activation in vivo

To investigate the effect of ALRF on neutrophil recruitment *in vivo*, we performed intravital microscopy of the cremaster muscle in mice 10 hours after bilateral nephrectomy or sham operated control animals. Neutrophil rolling was assessed as leukocyte rolling flux fraction, which is defined as the number of rolling leukocytes divided by the total number of leukocytes passing through the same vessel (26). During the first hour after exteriorization of the cremaster muscle, rolling flux fraction was not different between sham mice and mice with ALRF (Figure 1A). Neutrophil rolling during that time was almost exclusively P-selectin dependent, because it was completely blocked by the anti-P-selectin mAb RB40.34 (data not shown). However, the rolling velocity of neutrophils from mice with ALRF was significantly elevated compared to control neutrophils (Figure 1B). The number of adherent cells in mice with ALRF was significantly reduced compared to sham mice (Figure 1C). Hemodynamic parameters for both groups are presented in Table 1 and show no significant differences in white blood cell count, vessel diameter, blood flow velocity, and shear rate.

ALRF does not affect chemokine-induced arrest of neutrophils in vivo

In order to unveil the influence of ALRF on chemokine-induced arrest, mice were injected with CXCL1 and the number of adherent cells was determined. Injection of the recombinant murine chemokine CXCL1, which binds to and activates CXCR2, induced immediate firm arrest in sham mice (Figure 2). Mice with ALRF showed the same number of adherent neutrophils under baseline conditions and the same increase of adherent cells after CXCL1 injection compared to sham mice (Figure 2). Wall shear rates and diameters were similar in the investigated venules, excluding a hemodynamic contribution to reduced neutrophil adhesion (data not shown).

ALRF alters the immune response during LPS-induced inflammation

Neutrophil recruitment is a hallmark feature of the innate immune response. In order to induce inflammation, LPS was injected intrascrotally 4h before intravital microscopy. Mice with ALRF displayed an increased rolling flux fraction (Figure 3A), elevated neutrophil rolling velocity (Figure 3B), and reduced number of intravascular adherent cells compared to sham operated animals (Figure 3C). As in this model neutrophil rolling is P- and E-selectin mediated (data not shown), we blocked P-selectin by a monoclonal antibody to isolate E-selectin mediated neutrophil rolling. The rolling velocity of neutrophils from mice with ALRF on E-selectin *in vivo* was significantly elevated compared to control neutrophils (Figure 3D). These data suggest that ALRF alters the immune response during LPS-induced inflammation.

To exclude differences in the expression levels of adhesion molecules on endothelial cells from sham mice and ALRF mice, we analyzed the surface expression of ICAM-1, P-selectin, and E-selectin on endothelial cells of the cremaster muscle by flow cytometry. Endothelial cells from sham mice and ALRF mice expressed similar levels of adhesion molecules (ICAM-1, P-selectin, E-selectin) after LPS stimulation (Supplemental Figure 1).

Hemodynamic parameters for both groups are presented in Table 1 and show no significant differences in white blood cell count, vessel diameter, blood flow velocity, and shear rate.

ALRF reduces neutrophil transmigration in vivo

The reflected light oblique transillumination (RLOT) microscopy technique was used to assess neutrophil extravasation after LPS application using intravital microscopy. 10 hours after bilateral nephrectomy mice showed a significantly reduced number of transmigrated

neutrophils into the tissue after LPS stimulation (Figure 4A). Representative reflected light oblique transillumination microscopic images of sham mice and mice with ALRF 4 h after LPS application are shown in 4 B and C, respectively. By using whole-mount confocal immunofluorescence staining of the LPS-stimulated cremaster muscle, we were able to show that almost all intravascular and extravascular cells were $CD45^+$ and that over 90% of these leukocytes within LPS pretreated venules were neutrophils (Figure 4D). As chemokine induced arrest was not affected by ALRF, these data suggest that ALRF affects selectin-mediated neutrophil rolling as well as neutrophil transmigration.

ALRF completely abolishes selectin-mediated slow rolling

To further investigate the effect of ALRF on selectin-mediated slow neutrophil rolling on defined substrates, we performed autoperfused flow chamber assays. The advantage of this system is that neutrophils can be investigated in whole blood. This is important, because isolated neutrophils express increased levels of Mac-1 and show a decreased ability to roll, especially under high shear stress (27–29).

Flow chambers were coated with either a selectin alone (E- or P-selectin) or a selectin in combination with ICAM-1. The flow chambers were perfused with blood from mice 10 hours after nephrectomy or sham operation and the rolling velocity was determined. The rolling velocities of neutrophils from sham operated mice rolling on P-selectin/ICAM-1 (Figure 5A) or E-selectin/ICAM-1 (Figure 5B) were significantly reduced compared to the rolling velocities on E-selectin (Figure 5A) alone or P-selectin (Figure 5B) alone, respectively. Neutrophils from mice with ALRF showed similar rolling velocities on P-selectin (Figure 5A) and E-selectin (Figure 5B) as control neutrophils but failed to reduce their rolling velocities on P-selectin/ICAM-1 (Figure 5A) and E-selectin/ICAM-1 (Figure 5B).

ALRF causes altered intracellular signaling and reduces transmigration in vitro

In order to exclude that altered expression levels of adhesion molecules were responsible for the abolished slow neutrophil rolling, we measured the expression levels of adhesion molecules on neutrophils by using flow cytometry. There were no differences of the expression levels of PSGL-1, LFA-1, and Mac-1 on the surface of neutrophils from mice with ALRF and control mice (Figure 6A and Supplemental Figure 2A).

In order to investigate whether the reduced number of transmigrated cells seen *in vivo* was a consequence of reduced adhesion or diminished transmigration, we performed an *in vitro* transmigration assay using a transwell systems with IL-1β-stimulated bEND.5 endothelial cells. Incubation of endothelial cells with plasma from mice with ALRF did not influence the transmigration of control neutrophils (Figure 6B). However, the number of transmigrated neutrophils from mice with ALRF through endothelial cells pretreated with plasma from control mice or mice with ALRF was significantly reduced (Figure 6B), suggesting that ALRF reduces transmigration by affecting neutrophils, but not endothelial cells.

Selectin engagement leads to activation of an immunoreceptor tyrosine-based activation motif (ITAM)-dependent pathway, which in turn activates the spleen tyrosine kinase (Syk) (17–20). The signaling pathway downstream of Syk divides into a phospholipase C (PLC) γ2- and phosphoinositide 3-kinase (PI3K) γ-dependent pathway (19). p38 MAPK is located downstream of PLCγ2 (19). In order to reveal the molecular mechanism of the abolished selectin-mediated slow neutrophil rolling in neutrophils from mice with ALRF, we investigated the phosphorylation of Syk, Akt (as a readout for PI3K activation), PLCγ2, and p38 MAP kinase. Phosphorylation of Syk (Figure 6C, Supplemental Figure 3A), Akt (Figure 6C, Supplemental Figure 3B), PLCγ2 (Figure 6C, Supplemental Figure 3C), and p38 (Figure

6C, Supplemental Figure 3D) could be detected in control neutrophils after E-selectin stimulation, whereas phosphorylation of these molecules was reduced in E-selectin-stimulated neutrophils isolated from mice with ALRF (Figure 6C, Supplemental Figure 3A–D). This data suggest that ALRF inhibits selectin-mediated integrin activation by interfering with intracellular signaling pathways.

Selectin-mediated slow leukocyte rolling is abrogated in patients with sepsis-induced AKI

To investigate the effect of ALRF on selectin-mediated slow neutrophil rolling, we conducted a prospective observational study in critically-ill patients suffering from either sepsis alone or sepsis in combination with acute kidney injury (AKI). 15 Patients (5 with Sepsis, 5 with sepsis-induced AKI, 5 healthy volunteers) were included in this study and analyzed. There were no significant differences regarding demographic data, APACHE II score, SAPS score, and SOFA score between the sepsis and the sepsis-induced AKI group (Table 2). At the time of enrolment, no patient received renal replacement therapy; all patients with sepsis-induced AKI were classified as RIFLE-F. Similar to our findings in mice, expression levels of the adhesion molecules PSGL-1, LFA-1, and L-selectin were similar among the different groups (Figure 7A and Supplemental Figure 2B). To investigate the rolling velocity of neutrophils from critically ill patients with and without AKI, we used a recently published flow chamber system (16). Neutrophils from healthy volunteers (control patients) and patients suffering from sepsis showed a significantly reduced rolling velocity on P-selectin/ICAM-1 (Figure 7B) and E-selectin/ICAM-1 (Figure 7C) compared to P-selectin alone (Figure 7B) and E-selectin (Figure 7C) alone, respectively. However, neutrophils from patients with sepsis-induced AKI showed completely abolished selectin-mediated slow rolling on P-selectin/ICAM-1 (Figure 7B) and E-selectin/ICAM-1 (Figure 7C), suggesting that AKI interferes with intracellular signaling pathways in neutrophils.

To confirm our data *in vitro* and extend our findings to monocytes, we isolated neutrophils and monocytes, incubated the cells with plasma from different patients (control, sepsis, AKI) and determined the rolling velocity. Incubating isolated neutrophils in plasma from patients with sepsis-induced AKI abolished slow leukocyte rolling on E-selectin/ICAM-1 and P-selectin/ICAM-1 (Figure 7D–E). Likewise, incubating isolated monocytes in plasma from patients with sepsis-induced AKI abolished slow leukocyte rolling on E-selectin/VCAM-1 and P-selectin/VCAM-1 (Figure 7F+G).

Discussion

AKI in critically ill patient remains a great clinical challenge, in particular in patients with sepsis-induced AKI. AKI increases both morbidity and in-hospital mortality (2, 3). The mechanisms by which AKI exerts its detrimental effects remain unknown. However, current belief holds that the negative effects of AKI extend beyond fluid overload and electrolyte abnormalities. Using a translational approach, we here show that ALRF inhibits neutrophil recruitment by abolishing selectin-induced slow rolling and decreasing transendothelial migration. These effects appear to be mediated by altered intracellular signaling rather than by changes in surface molecule expression.

We have previously shown that ALRF impairs recruitment of neutrophils into the inflamed lung and thereby attenuates aseptic, inflammatory lung injury (6). These effects seem to rest largely with neutrophils, as only neutrophils isolated from mice with ALRF but not normal neutrophils in plasma from mice with ALRF demonstrated impaired pulmonary recruitment. So far, most studies addressing the effects of ALRF on neutrophil function have been in the context of chronic kidney disease (CKD) (30, 31). These studies have identified several defects in neutrophils during CKD, including decreased superoxide production and

phagocytosis as well as enhanced apoptosis. Contrary, ALRF does not seem to affect superoxide production and apoptosis (6).

To further study the underlying mechanisms, we first used intravital microscopy of the mouse cremaster muscle. We studied neutrophil recruitment in normal mice, mice pre-treated with LPS, mice with ALRF, and mice with ALRF pre-treated with LPS.

ALRF had no effect on microvasculatory hemodynamics. However, ALRF significantly increased neutrophil rolling velocity and reduced the number of adherent cells but did not affect chemokine-induced arrest. In the setting of LPS-induced tissue inflammation, ALRF exerted similar effects. The neutrophil rolling velocity was significantly higher, whereas the number of adhering cells was significantly lower.

Using both *in vivo* and *in vitro* transmigration assays, we found that ALRF also impairs transendothelial migration of neutrophils. Similar to our previous studies (6), this effect seemed to rest with neutrophils isolated from mice with ALRF rather than with plasma obtained from mice with ALRF. Only neutrophils from mice with ALRF but not normal neutrophils displayed impaired transmigration across inflamed endothelial cells. Furthermore, we showed that incubating endothelial cells with plasma from mice with ALRF did not affect the transmigration of normal neutrophils.

At first sight, our previous and current results appear to contradict other studies describing increased neutrophil recruitment into remote organs during AKI (6, 32–34). These studies have largely investigated the effects of AKI on remote healthy organs and cannot explain the increased incidence of bacterial infection and/or bacteremia in patients with AKI. By contrast, our studies exclusively describe neutrophil recruitment into inflamed organs. Here, the cremaster muscle undergoes inflammatory changes either as a result of tissue preparation (trauma) or tissue trauma plus LPS-injection. One can therefore speculate that AKI induces remote neutrophil recruitment under non-inflammatory conditions but decreases remote leukocyte recruitment under inflammatory conditions. As neutrophils are crucial for control and elimination of bacterial infections (35), our findings allow us to hypothesize that impaired selectin-mediated integrin activation and transmigration during AKI contributes to the increased incidence of bacterial infections in patient with AKI.

Our results have allowed us to further hypothesize that ALRF abolishes selectin-mediated slow neutrophil rolling. To further test this hypothesis, we studied the rolling of normal and ALRF neutrophils in an autoperfused flow chamber assay. Normal and ALRF neutrophils demonstrated similar rolling velocities on P-selectin and E-selectin. ALRF neutrophils, however, did not display reduced rolling velocities on P-selectin/ICAM-1 or E-selectin/ICAM-1. In the intravital microscopy experiments, the difference in the rolling velocity between control and ALRF neutrophils can be explained by the fact that endothelial cells express selectins and integrin ligands (Supplemental Figure 1). These data suggest that the signaling pathway linking PSGL-1 to integrin activation is disturbed. It has been demonstrated that this pathway is important for $G\alpha_i$-independent neutrophil recruitment (17, 19, 20).

Leukocyte adhesion molecules, including selectins and their ligands, play a pivotal role in leukocyte recruitment (15). Nonetheless, we could not detect changes in surface expression of three major adhesion molecules on neutrophils.

Since ALRF drastically affects selectin-dependent neutrophil rolling, we next investigated the intracellular, selectin-dependent signaling pathways. Both the PI3Kγ- and PLCγ2-dependent pathways and their phosphorylation are crucial for neutrophil recruitment (19). Whereas we could find E-selectin-stimulated phosphorylation in normal neutrophils, we

could not detect E-selectin-stimulated phosphorylation in neutrophils isolated from mice with ALRF. We therefore hypothesize that ALRF inhibits selectin-mediated integrin activation by means of interference with intracellular signaling pathways and thereby ultimately impairs slow neutrophil rolling.

Finally, we validated our animal data in neutrophils from septic patients with or without AKI. AKI did not affect the expression of PSGL-1, LFA-1, and L-selectin. Similar to our animal data, AKI also failed to reduce neutrophil rolling velocities on P-selectin/ICAM-1 and on E-selectin/ICAM-1 in septic patients with AKI.

Impaired renal function during AKI results in the retention of various non-nitrogenous and nitrogenous waste products, metabolic acidosis, hyperkalemia, and hypervolemia. This is associated with other severe metabolic disturbances such as massively increased oxidative stress, reduced adsorptive, excretory and metabolic capacity of the kidneys, and hyperglycemia (36, 37). However, the exact mechanism how uremia and which toxins affect PSGL-1 mediated signaling and transmigration is unknown.

To this end, our data show that acute loss of renal function significantly impairs neutrophil rolling and transmigration, but not chemokine-induced arrest, both *in vivo* and *in vitro*. These effects appear to be, at least partially, due to decreased phosphorylation of selectin-dependent intracellular signaling. Our data further support the concept of AKI-induced anti-inflammatory effects both in mice and men.

Methods

Animals

We used C57BL/6 wild-type mice (WT mice, 2–3 months old, 20–32 g of body weight, Charles River Laboratories, Wilmington, MA). Mouse colonies were maintained under specific pathogen-free conditions. All experiments were approved by local government authorities and were in agreement with the National Institutes of Health Guide for the Care and Use of Laboratory Animals.

Observational study

In order to investigate the effect of ALRF on selectin-mediated slow neutrophil rolling, we conducted a prospective observational study in critically-ill patients suffering from either sepsis alone or sepsis with AKI (RIFLE-F). The study was approved by the local ethic committee of the University of Münster (Institutional Review Board). We obtained informed consent prior to enrollment. Exclusion criteria from the study were age < 18 years, pregnancy, immunosuppressive therapy within the last 7 days, chronic renal insufficiency, pre-existing hematologic diseases and HIV-infection. Sepsis was defined according to the American College of Chest Physicians/Society of Critical Care Medicine consensus conference definitions by infection plus two systemic inflammatory response syndrome criteria (38), whereas AKI was defined according to the RIFLE criteria (39).

Reagents

Unlike otherwise stated, all reagents were obtained from Sigma Aldrich (Taufkirchen, Germany).

Murine model of ALRF

Mice were anesthetized and ALRF was achieved as described previously (6). Control animals scheduled for sham operation received the same surgical procedure with the exception that the pedicels were not ligated and the kidneys left in situ. We previously

demonstrated that mice developed ALRF 10 hours after bilateral nephrectomy, which was measured as a significant increase in serum creatinine and urea nitrogen levels (6).

Intravital microscopy

Ten hours after nephrectomy or sham operation, intravital microscopy of the cremaster muscle of the mouse was performed as described previously (17, 19, 20, 40). Some mice were injected intrascrotally with 0.5 μg/kg LPS from E. coli 4 hours before preparation. In order to investigate chemokine-induced arrest, CXCL1 (Peprotech, Rocky Hill, NJ, USA) was injected intravenously after preparing the cremaster muscle and the number of adherent cells was determined. The parameters of neutrophil rolling velocity and neutrophil arrest were determined by transillumination microscopy (17, 19, 20, 40). Leukocyte rolling flux fraction was calculated as a percentage of total leukocyte flux (26). Neutrophil transmigration was investigated using the reflected light oblique transillumination (RLOT) microscopy technique as described previously (41).

Cremaster whole mount staining

After sham operation or nephrectomy and LPS injection, mice were sacrificed and the scrotum was opened to expose the cremaster muscle. The cremaster was prepared as described previously (42) and samples were incubated with different antibodies (rat anti-mouse PECAM1-antibody (clone V1G5.1), rabbit anti-mouse MRP14-antibody, and rat anti-mouse CD45-PerCP-antibody (clone 30-F11)). Samples were mounted on glass slides and fluorescence images were obtained with a Zeiss LSM510meta confocal microscope (Zeiss, Oberkochen, Germany).

Autoperfused murine flow chamber

We used an autoperfused murine blood flow chamber system to investigate the rolling velocity of neutrophils in whole blood, as described previously (17, 19, 20). It has been shown that over 90% of the rolling cells in the autoperfused flow chamber are neutrophils (43). Flow chamber experiments were performed 10 hours after nephrectomy or sham operation.

Blood-perfused human microflow chamber

We used the blood perfused human microflow chamber assay as described previously (16). More than 90% of cells in the microfluidic whole human blood perfusion system were neutrophils (16).

For some experiments, neutrophils or monocytes were isolated from human whole blood. Monocytes were isolated from whole blood following a previously published protocol (purity of isolated monocytes > 90%, data not shown) (44). Neutrophils were isolated from whole blood by using a Histopaque gradient (purity of isolated neutrophils > 90%, data not shown).

After isolation, cells were resuspended in human control serum or serum obtained from patients with either sepsis or sepsis-induced AKI and incubated for 30 minutes. For microflow chamber experiments with isolated neutrophils, glass capillaries were coated with E-selectin (3,5 μg/ml), P-selectin (20μg/ml), E-selectin/ICAM-1 (3,5/3,5 μg/ml) or P-selectin/ICAM-1 (20/5 μg/ml) for 2 hours. Glass capillaries for microflow chamber assays with isolated human monocytes were coated with E-selectin (7,5 μg/ml), P-selectin (50μg/ml), E-selectin/VCAM-1 (7,5/10 μg/ml) or P-selectin/VCAM-1 (50/30 μg/ml) for 2 hours. Chambers were blocked with casein 1% (Fisher Scientific, Waltham, MA, USA) for 1 hour.

In vitro transmigration assay

Transendothelial migration of bone marrow–derived neutrophils through cultured endothelioma cells was performed as previously described (42). Briefly, a total of 5×10^4 bEnd.5 cells/well of 6.5-mm transwells (Corning Life Sciences), coated with 50 μg/mL laminin (Boehringer Mannheim), were grown for 2 days and stimulated 16 hours before the assay with IL-1β at 10 ng/ml (Peprotech, Rocky Hill, NJ, USA) for 16 hours. 4 hours before the experiment, the endothelial cell layer was pre-treated with plasma obtained from mice 10 hours after bilateral nephrectomy or sham operated control mice. After washing away the plasma, 5×10^5 isolated neutrophils were added per transwell. Transmigration was allowed for 1 hour. The number of transmigrated cells in the well was counted.

FACS-analysis of neutrophils from human whole blood

We analyzed the surface expression of leukocyte adhesion molecules on human and mouse neutrophils by using FACS. Isolated neutrophils were incubated with different antibodies (anti-human PSGL1-antibody, clone KPL-1, BD Biosciences, Franklin Lakes, NJ, USA; anti-human LFA1-antibody, clone MEM-25, ImmunoTools, Friesoythe, Germany; anti-human L-Selectin-antibody, clone LT-TD180, ImmunoTools, Friesoythe, Germany; anti-mouse Mac-1-antibody, clone M1/70, BD Biosciences, Franklin Lakes, NJ, USA; anti-mouse LFA-1-antibody, clone M17/4, BD Biosciences, Franklin Lakes, NJ, USA; anti-mouse PSGL-1-antibody, clone 4RB12, purified from hybridoma culture) for 20 minutes. Samples were analyzed using a FACSCanto flow cytometer (BD Biosciences, Franklin Lakes, NJ, USA). FACS data was processed using FlowJo (version 7.5.5; Tree Star Inc., Ashland, OR, USA).

FACS Analysis of endothelial adhesion molecules in the cremaster muscle

After sham operation or nephrectomy and LPS application, the mice were sacrificed and the cremaster muscle was removed, minced and incubated with an enzyme cocktail containing DNAse, collagenase and hyaluronidase at 37°C for 60 minutes. The tissue was passed through a 70μm cell strainer (BD Biosciences, Franklin Lakes, NJ, USA), washed and incubated with FC-block (clone 2.4GL) for 20 minutes. The cells were stained with rat anti-mouse CD45-PerCP antibody (clone 30-F11), rat anti-mouse CD41-PE antibody (clone MWReg30), rat anti-mouse CD31-FITC antibody (clone MEC 13.3), rat anti-mouse CD62P–FITC antibody (clone RB40.34), goat anti-mouse CD31 antibody (clone M-20), goat anti-mouse CD54 antibody (clone M-19), rat anti-mouse CD62E–Alexa633 antibody (clone 9A9) and Alexa-633 labelled donkey anti-goat secondary antibody. Endothelial cells were identified by gating on CD31-positive cells and excluding CD41- and CD45-positive cells in a second gating step.

Western blotting

For biochemical assays, isolated bone-marrow derived neutrophils from sham mice or mice 10 hours after bilateral nephrectomy were stimulated with immobilized E-selectin as described previously (17, 19). Following stimulation, cells were lysed using RIPA buffer (17). Lysate was boiled with Laemmli sample buffer at 95°C for 10 minutes, run on a 10% PAGE-SDS gel and immunoblotted with antibodies against Syk, Akt, phosphor-Akt, PLCγ2, phospho-PLCγ2, p38 MAP kinase and phospho-p38 MAP kinase (all from Cell Signaling Technology, Danvers, MA, USA). Blots were developed using the Amersham ECL Plus detection system (GE Healtcare, Piscataway, NJ, USA).

Statistics

Statistical analysis was performed with PASW (version 18.0) using one-way ANOVA, Student-Newman-Keuls test, post-hoc correction or t-test where appropriate. All data are represented as means ± SEM. A p-value <0.05 was taken as statistically significant.

Supplementary Material

Refer to Web version on PubMed Central for supplementary material.

Acknowledgments

This study was supported by grants from the German Research Foundation (AZ 428/3-1 to A.Z.), German Interdisciplinary Association of Critical Care Medicine (to A.Z.), and the NIH (5K08GM081459-03 to KS).

References

1. Chertow GM, Burdick E, Honour M, et al. Acute kidney injury, mortality, length of stay, and costs in hospitalized patients. J Am Soc Nephrol. 2005; 16:3365–3370. [PubMed: 16177006]
2. Bagshaw SM, Uchino S, Bellomo R, et al. Septic acute kidney injury in critically ill patients: clinical characteristics and outcomes. Clin J Am Soc Nephrol. 2007; 2:431–439. [PubMed: 17699448]
3. Uchino S, Kellum JA, Bellomo R, et al. Acute renal failure in critically ill patients: a multinational, multicenter study. JAMA. 2005; 294:813–818. [PubMed: 16106006]
4. Thadhani R, Pascual M, Bonventre JV. Acute renal failure. N Engl J Med. 1996; 334:1448–1460. [PubMed: 8618585]
5. de Mendonca A, Vincent JL, Suter PM, et al. Acute renal failure in the ICU: risk factors and outcome evaluated by the SOFA score. Intensive Care Med. 2000; 26:915–921. [PubMed: 10990106]
6. Zarbock A, Schmolke M, Spieker T, et al. Acute uremia but not renal inflammation attenuates aseptic acute lung injury: a critical role for uremic neutrophils. J Am Soc Nephrol. 2006; 17:3124–3131. [PubMed: 17035612]
7. Lewis SL, Van Epps DE. Neutrophil and monocyte alterations in chronic dialysis patients. Am J Kidney Dis. 1987; 9:381–395. [PubMed: 3555014]
8. Jaber BL, Cendoroglo M, Balakrishnan VS, et al. Apoptosis of leukocytes: basic concepts and implications in uremia. Kidney Int Suppl. 2001; 78:S197–S205. [PubMed: 11169011]
9. Ratter F, Germer M, Fischbach T, et al. S-adenosylhomocysteine as a physiological modulator of Apo-1-mediated apoptosis. Int Immunol. 1996; 8:1139–1147. [PubMed: 8757959]
10. Takagi T, Chung TG, Saito A. Determination of polyamines in hydrolysates of uremic plasma by high-performance cation-exchange column chromatography. J Chromatogr. 1983; 272:279–285. [PubMed: 6833425]
11. De Waele JJ, Hoste EA, Blot SI. Blood stream infections of abdominal origin in the intensive care unit: characteristics and determinants of death. Surg Infect (Larchmt). 2008; 9:171–177. [PubMed: 18426349]
12. Hoste EA, Blot SI, Lameire NH, et al. Effect of nosocomial bloodstream infection on the outcome of critically ill patients with acute renal failure treated with renal replacement therapy. J Am Soc Nephrol. 2004; 15:454–462. [PubMed: 14747393]
13. Thakar CV, Yared JP, Worley S, et al. Renal dysfunction and serious infections after open-heart surgery. Kidney Int. 2003; 64:239–246. [PubMed: 12787415]
14. Tumbarello M, Spanu T, Caira M, et al. Factors associated with mortality in bacteremic patients with hematologic malignancies. Diagn Microbiol Infect Dis. 2009; 64:320–326. [PubMed: 19345033]
15. Ley K, Laudanna C, Cybulsky MI, et al. Getting to the site of inflammation: the leukocyte adhesion cascade updated. Nat Rev Immunol. 2007; 7:678–689. [PubMed: 17717539]

16. Kuwano Y, Spelten O, Zhang H, et al. Rolling on E- or P-selectin induces the extended but not high-affinity conformation of LFA-1 in neutrophils. Blood. 116:617–624. [PubMed: 20445017]
17. Zarbock A, Abram CL, Hundt M, et al. PSGL-1 engagement by E-selectin signals through Src kinase Fgr and ITAM adapters DAP12 and FcR gamma to induce slow leukocyte rolling. J Exp Med. 2008; 205:2339–2347. [PubMed: 18794338]
18. Yago T, Shao B, Miner JJ, et al. E-selectin engages PSGL-1 and CD44 through a common signaling pathway to induce integrin alphaLbeta2-mediated slow leukocyte rolling. Blood. 2010; 116:485–494. [PubMed: 20299514]
19. Mueller H, Stadtmann A, Van Aken H, et al. Tyrosine kinase Btk regulates E-selectin-mediated integrin activation and neutrophil recruitment by controlling phospholipase C (PLC) gamma2 and PI3Kgamma pathways. Blood. 2010; 115:3118–3127. [PubMed: 20167705]
20. Zarbock A, Lowell CA, Ley K. Spleen tyrosine kinase Syk is necessary for E-selectin-induced alpha(L)beta(2) integrin-mediated rolling on intercellular adhesion molecule-1. Immunity. 2007; 26:773–783. [PubMed: 17543554]
21. Ley K. Arrest chemokines. Microcirculation. 2003; 10:289–295. [PubMed: 12851646]
22. Camps M, Carozzi A, Schnabel P, et al. Isozyme-selective stimulation of phospholipase C-beta 2 by G protein beta gamma-subunits. Nature. 1992; 360:684–686. [PubMed: 1465133]
23. Hirsch E, Katanaev VL, Garlanda C, et al. Central role for G protein-coupled phosphoinositide 3-kinase gamma in inflammation. Science. 2000; 287:1049–1053. [PubMed: 10669418]
24. Bokoch GM. Chemoattractant signaling and leukocyte activation. Blood. 1995; 86:1649–1660. [PubMed: 7654998]
25. Vestweber D. Adhesion and signaling molecules controlling the transmigration of leukocytes through endothelium. Immunol Rev. 2007; 218:178–196. [PubMed: 17624953]
26. Ley K, Gaehtgens P. Endothelial, not hemodynamic, differences are responsible for preferential leukocyte rolling in rat mesenteric venules. Circ Res. 1991; 69:1034–1041. [PubMed: 1934331]
27. Forsyth KD, Levinsky RJ. Preparative procedures of cooling and re-warming increase leukocyte integrin expression and function on neutrophils. J Immunol Methods. 1990; 128:159–163. [PubMed: 2324509]
28. Glasser L, Fiederlein RL. The effect of various cell separation procedures on assays of neutrophil function. A critical appraisal. Am J Clin Pathol. 1990; 93:662–669. [PubMed: 2327366]
29. Kuijpers TW, Tool AT, van der Schoot CE, et al. Membrane surface antigen expression on neutrophils: a reappraisal of the use of surface markers for neutrophil activation. Blood. 1991; 78:1105–1111. [PubMed: 1907873]
30. Sardenberg C, Suassuna P, Andreoli MC, et al. Effects of uraemia and dialysis modality on polymorphonuclear cell apoptosis and function. Nephrol Dial Transplant. 2006; 21:160–165. [PubMed: 16155068]
31. Anding K, Gross P, Rost JM, et al. The influence of uraemia and haemodialysis on neutrophil phagocytosis and antimicrobial killing. Nephrol Dial Transplant. 2003; 18:2067–2073. [PubMed: 13679482]
32. Ishii T, Doi K, Okamoto K, et al. Neutrophil elastase contributes to acute lung injury induced by bilateral nephrectomy. Am J Pathol. 177:1665–1673. [PubMed: 20709801]
33. Hoke TS, Douglas IS, Klein CL, et al. Acute renal failure after bilateral nephrectomy is associated with cytokine-mediated pulmonary injury. J Am Soc Nephrol. 2007; 18:155–164. [PubMed: 17167117]
34. Kim do J, Park SH, Sheen MR, et al. Comparison of experimental lung injury from acute renal failure with injury due to sepsis. Respiration. 2006; 73:815–824. [PubMed: 16960438]
35. Brown KA, Brain SD, Pearson JD, et al. Neutrophils in development of multiple organ failure in sepsis. Lancet. 2006; 368:157–169. [PubMed: 16829300]
36. Herget-Rosenthal S, Glorieux G, Jankowski J, et al. Uremic toxins in acute kidney injury. Semin Dial. 2009; 22:445–448. [PubMed: 19708999]
37. Himmelfarb J, McMonagle E, Freedman S, et al. Oxidative stress is increased in critically ill patients with acute renal failure. J Am Soc Nephrol. 2004; 15:2449–2456. [PubMed: 15339994]

38. American College of Chest Physicians/Society of Critical Care Medicine Consensus Conference: definitions for sepsis and organ failure and guidelines for the use of innovative therapies in sepsis. Crit Care Med. 1992; 20:864–874. [PubMed: 1597042]

39. Kellum JA, Bellomo R, Ronco C. The concept of acute kidney injury and the RIFLE criteria. Contrib Nephrol. 2007; 156:10–16. [PubMed: 17464110]

40. Zarbock A, Deem TL, Burcin TL, et al. Galphai2 is required for chemokine-induced neutrophil arrest. Blood. 2007; 110:3773–3779. [PubMed: 17699741]

41. Mempel TR, Moser C, Hutter J, et al. Visualization of leukocyte transendothelial and interstitial migration using reflected light oblique transillumination in intravital video microscopy. J Vasc Res. 2003; 40:435–441. [PubMed: 14530600]

42. Bixel MG, Li H, Petri B, et al. CD99 and CD99L2 act at the same site as, but independently of, PECAM-1 during leukocyte diapedesis. Blood. 116:1172–1184. [PubMed: 20479283]

43. Chesnutt BC, Smith DF, Raffler NA, et al. Induction of LFA-1-dependent neutrophil rolling on ICAM-1 by engagement of E-selectin. Microcirculation. 2006; 13:99–109. [PubMed: 16459323]

44. de Almeida MC, Silva AC, Barral A, et al. A simple method for human peripheral blood monocyte isolation. Mem Inst Oswaldo Cruz. 2000; 95:221–223. [PubMed: 10733742]

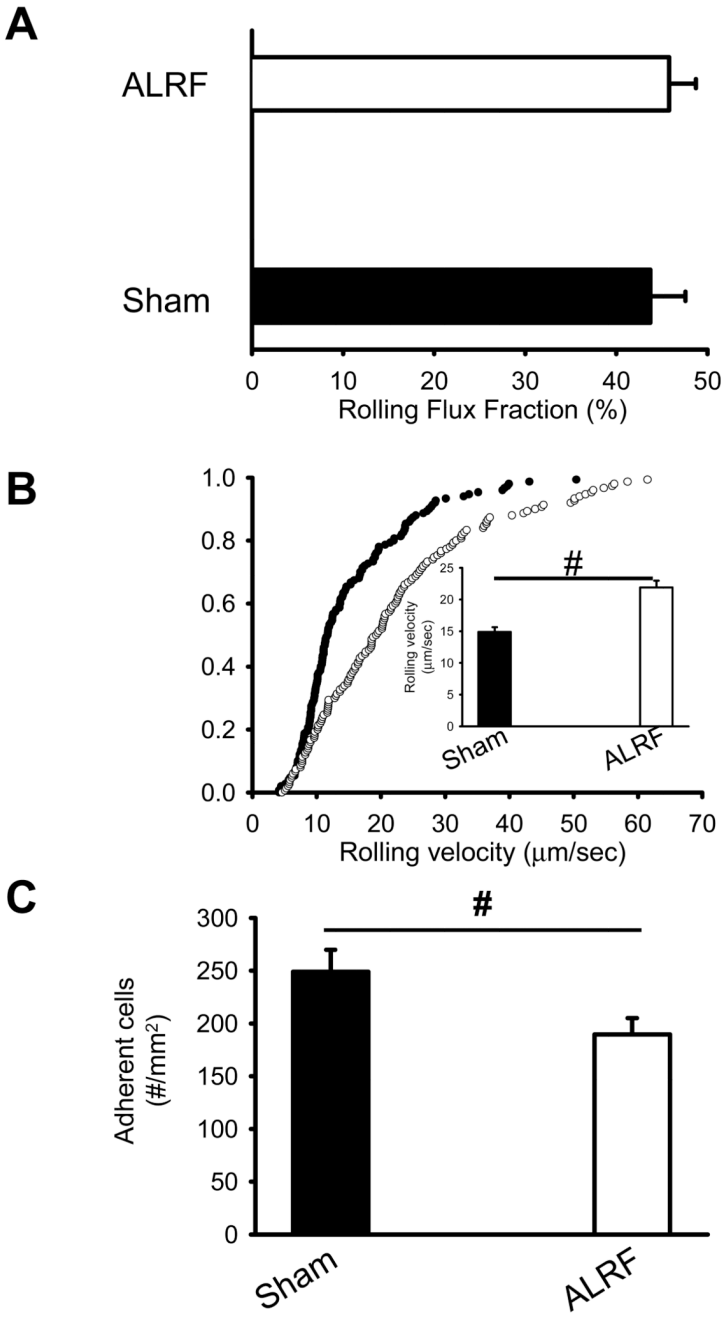

Figure 1. ALRF leads to inhibition of P-selectin mediated leukocyte activation *in vivo*

ALRF in mice was induced by bilateral nephrectomy 10 hours prior to intravital microscopy. (A) Leukocyte rolling flux fraction in untreated cremaster venules of mice with ALRF and sham-operated control mice (n=5). (B) Neutrophil rolling velocities in venules of mice with ALRF and sham-operated control mice. Data represent cumulative histograms of neutrophil rolling velocities measured after exteriorization of the cremaster muscle. The average rolling velocities (in µm/s) were calculated and are presented as means ± SEM (>100 neutrophils from 5 mice). (C) Numbers of adherent cells per mm^2 in murine cremaster muscle venules. The cremaster muscle was exteriorized 10 h after bilateral nephrectomy or sham operation (n=5). $^{\#}$ $p < 0.05$.

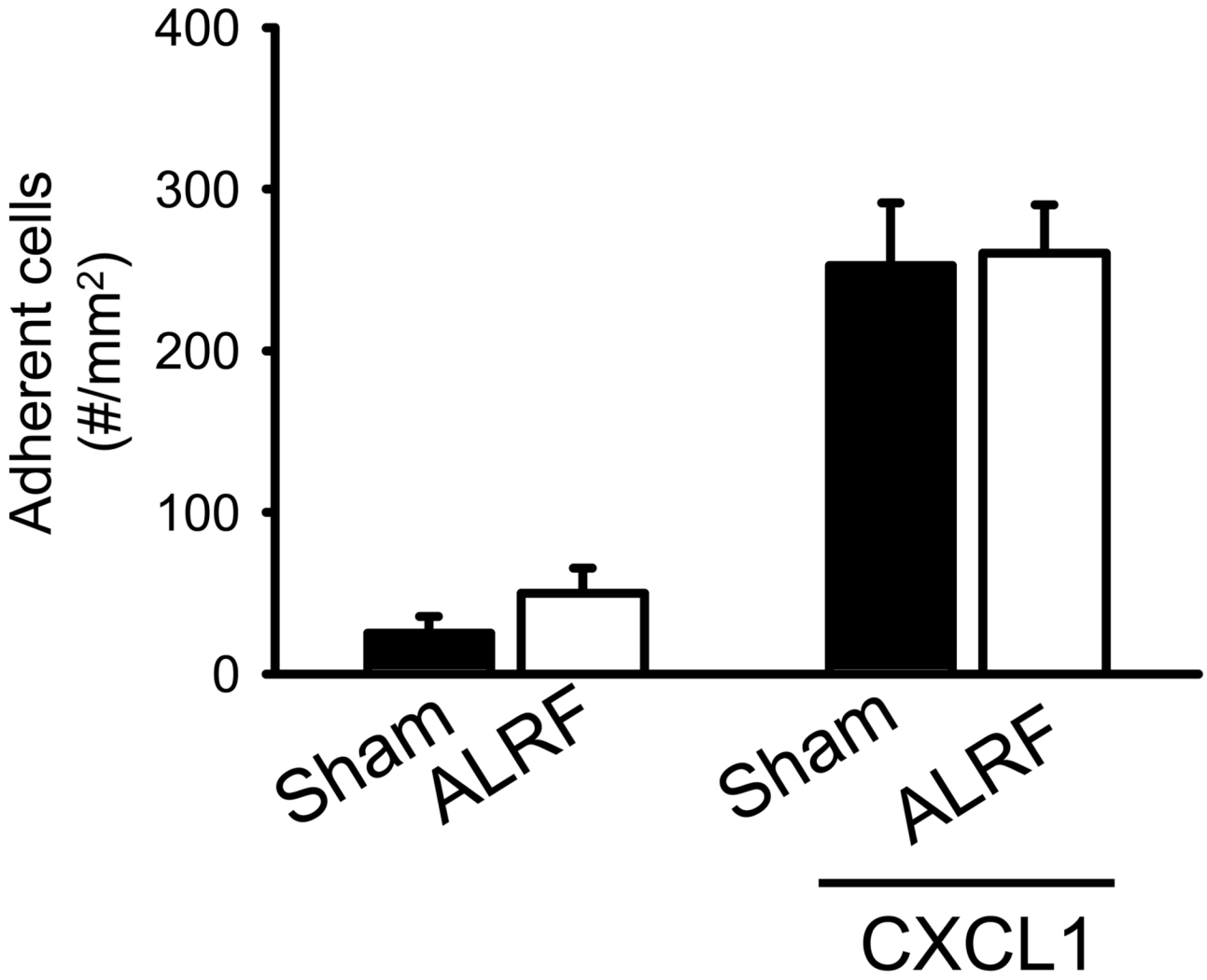

Figure 2. ALRF does not affect chemokine-induced arrest of leukocytes *in vivo*

Chemokine induced arrest of intravascular neutrophils in mice with ALRF and control mice was investigated after intravenous injection of 600ng CXCL1 by intravital microscopy of the cremaster muscle. The data was recorded and analyzed over the time period of 1 minute starting 15 seconds after the intravascular administration of CXCL1 (n=5). Data presented as means ± SEM.

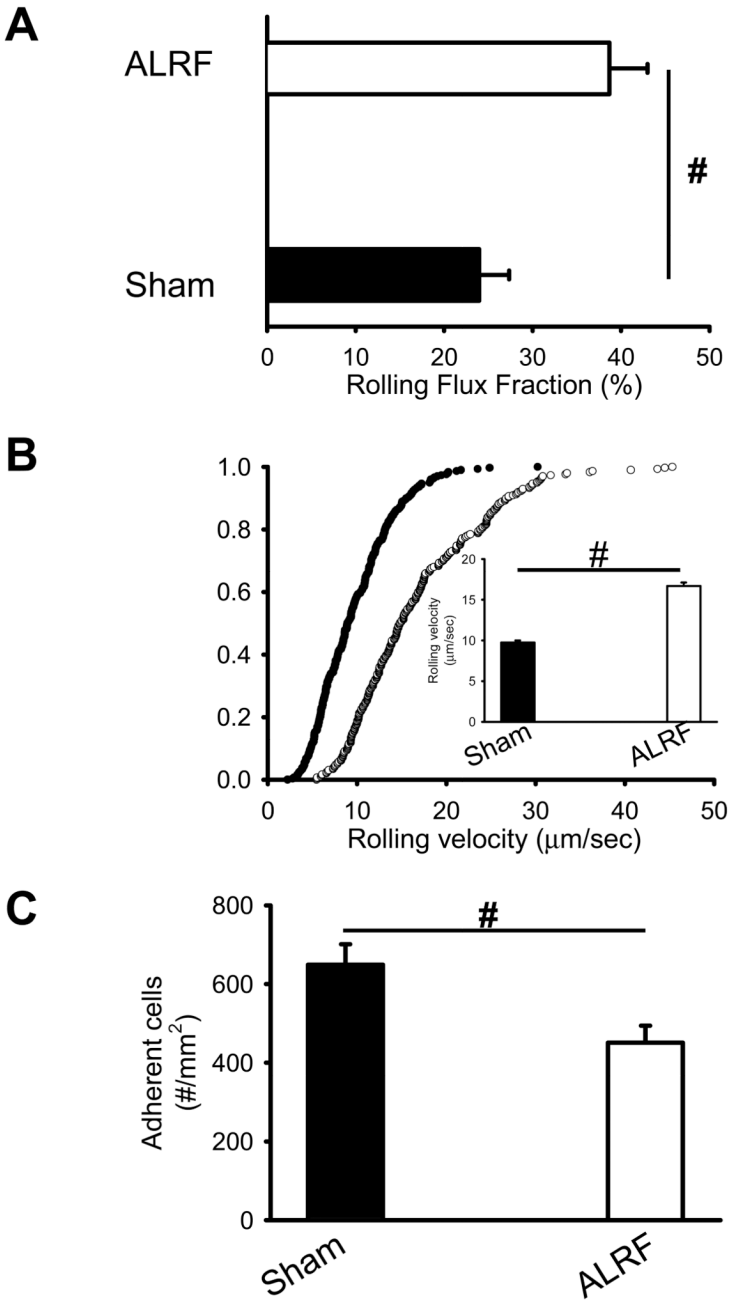

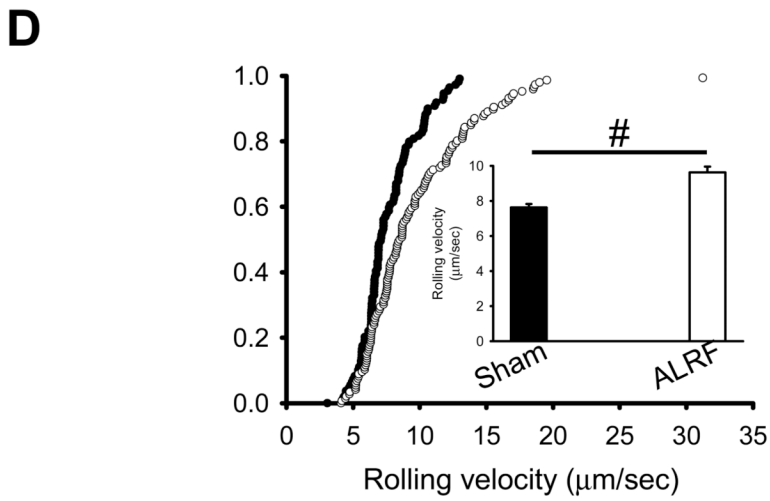

Figure 3. ALRF alters the immune response during LPS-induced inflammation

6h after bilateral nephrectomy or sham operation, LPS was injected intrascrotally in order to induce inflammation. Intravital microscopy was performed 4h after LPS injection. (A) Leukocyte rolling flux fraction in inflamed cremaster venules 4h after LPS injection (n=5). (B) Neutrophil rolling velocities in inflamed venules of mice with ALRF and control mice. Data represent cumulative histograms of neutrophil rolling velocities measured 4h after LPS injection. The average rolling velocities (in µm/s) were calculated and are presented as means ± SEM (>100 neutrophils from 5 mice). (C) Numbers of adherent cells per mm^2 in inflamed cremaster venules of mice with ALRF or control mice 4h after LPS injection (n=5). (D) After administration of a blocking antibody against P-selectin, the rolling velocity of neutrophils from mice with ALRF and sham operated control mice was determined. Data represent cumulative histograms of neutrophil rolling velocities measured 4h after LPS injection. The average rolling velocities (in µm/s) were calculated and are presented as means ± SEM (>100 neutrophils from 5 mice). $^{\#}$ $p < 0.05$.

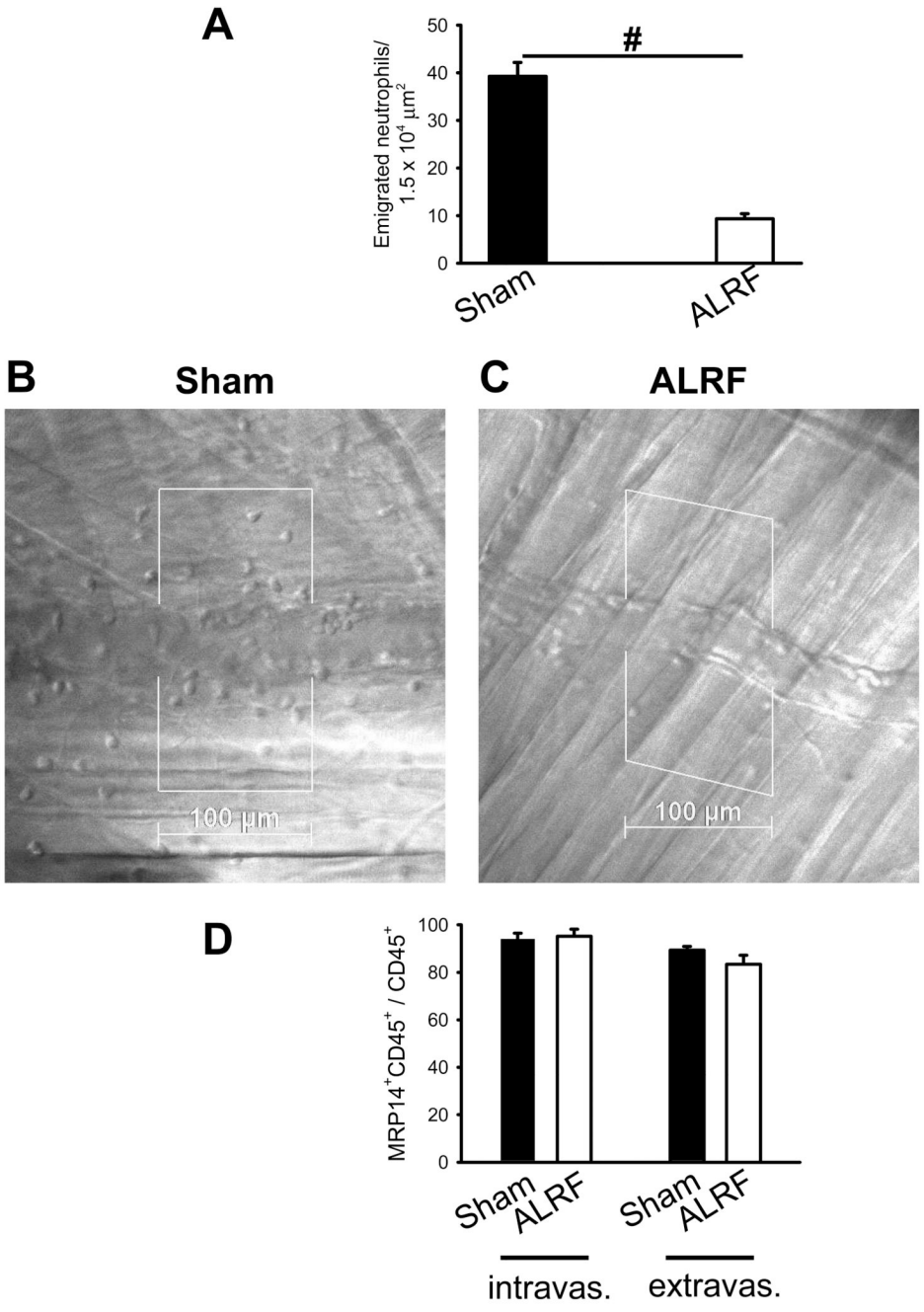

Figure 4. ALRF reduces neutrophil transmigration *in vivo*

Intravital microscopy was performed 10h after bilateral nephrectomy or sham operation. (A) Number of extravasated neutrophils in cremaster venules of LPS treated mice with ALRF or control mice per 1.5×10^4 µm^2 tissue area. The measurements were performed 4 h after intrascrotal LPS injection (n=5). (B + C) Representative reflected light oblique transillumination microscopic pictures of cremaster muscle postcapillary venules of control mice (B) or mice with ALRF 4 h after LPS injection (C). Demarcations on each side of the venule determine the areas in which extravasated neutrophils were counted. # $p < 0.05$. (D) Mice received LPS intrascrotally 6 hours after bilateral nephrectomy or sham operation. 4 hours after LPS application, mice were sacrificed, the cremaster was removed, fixed, stained

with PECAM1-, MRP14-, and CD45-antibodies and analyzed on a confocal microscope. The numbers of neutrophils ($MRP14^+CD45^+$) in the population of intravascular and extravascular leukocytes were counted and expressed as the percentage of $MRP14^+CD45^+$ cells within the CD45+ population (n=3).

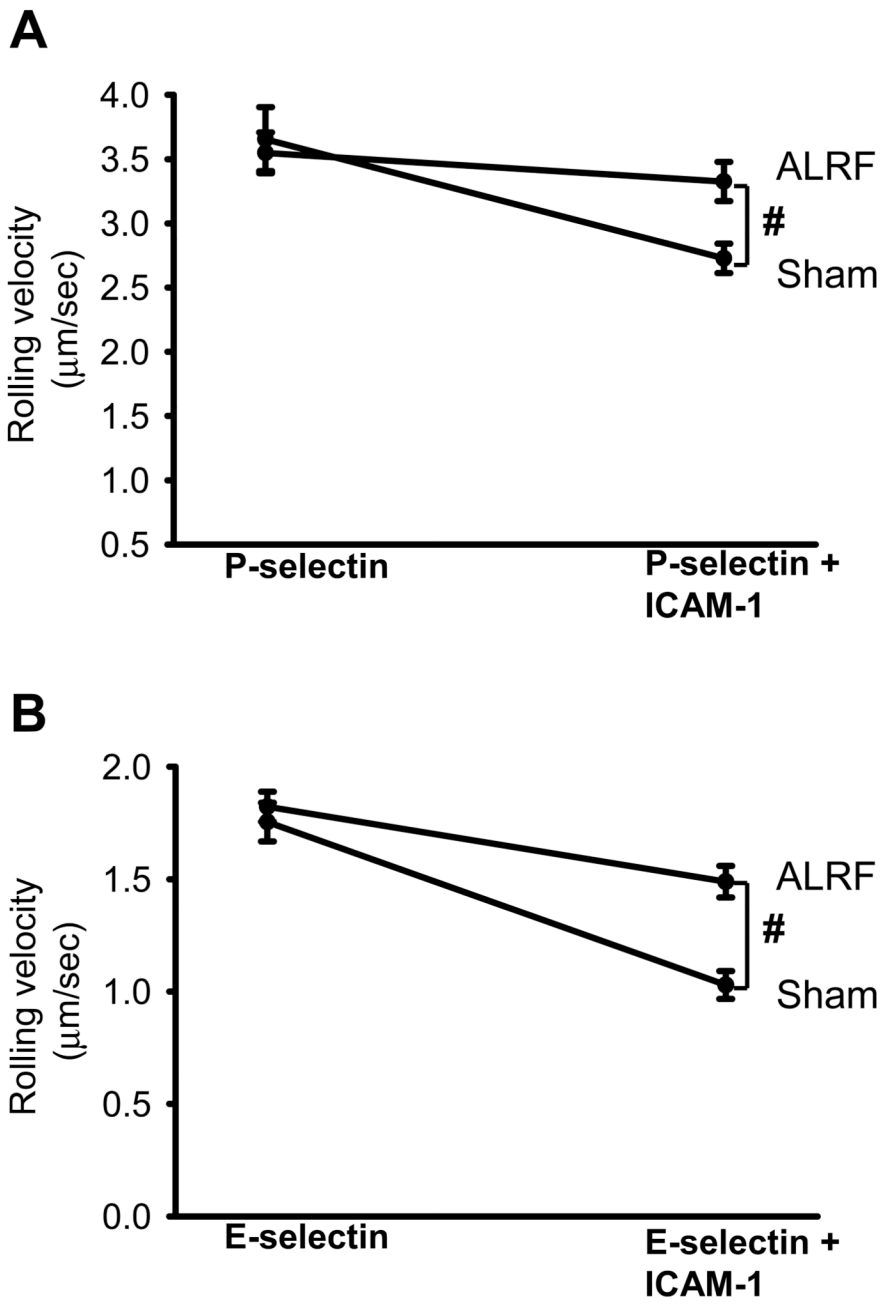

Figure 5. ALRF completely abolishes selectin-mediated slow rolling

(A + B) The carotid artery of control mice and mice with ALRF were cannulated with a catheter, which was connected to autoperfused flow chambers. (A) Average rolling velocity of neutrophils on P-selectin (left) and P-selectin/ICAM-1 (right) is presented as mean ± SEM (n=6–10). (B) Average rolling velocity of neutrophils on E-selectin (left) and E-selectin/ICAM-1 (right) is presented as mean ± SEM (n=6–10). The wall shear stress in all flow chamber experiments was 5–6 dynes/cm^2. $^{\#}$ $p < 0.05$.

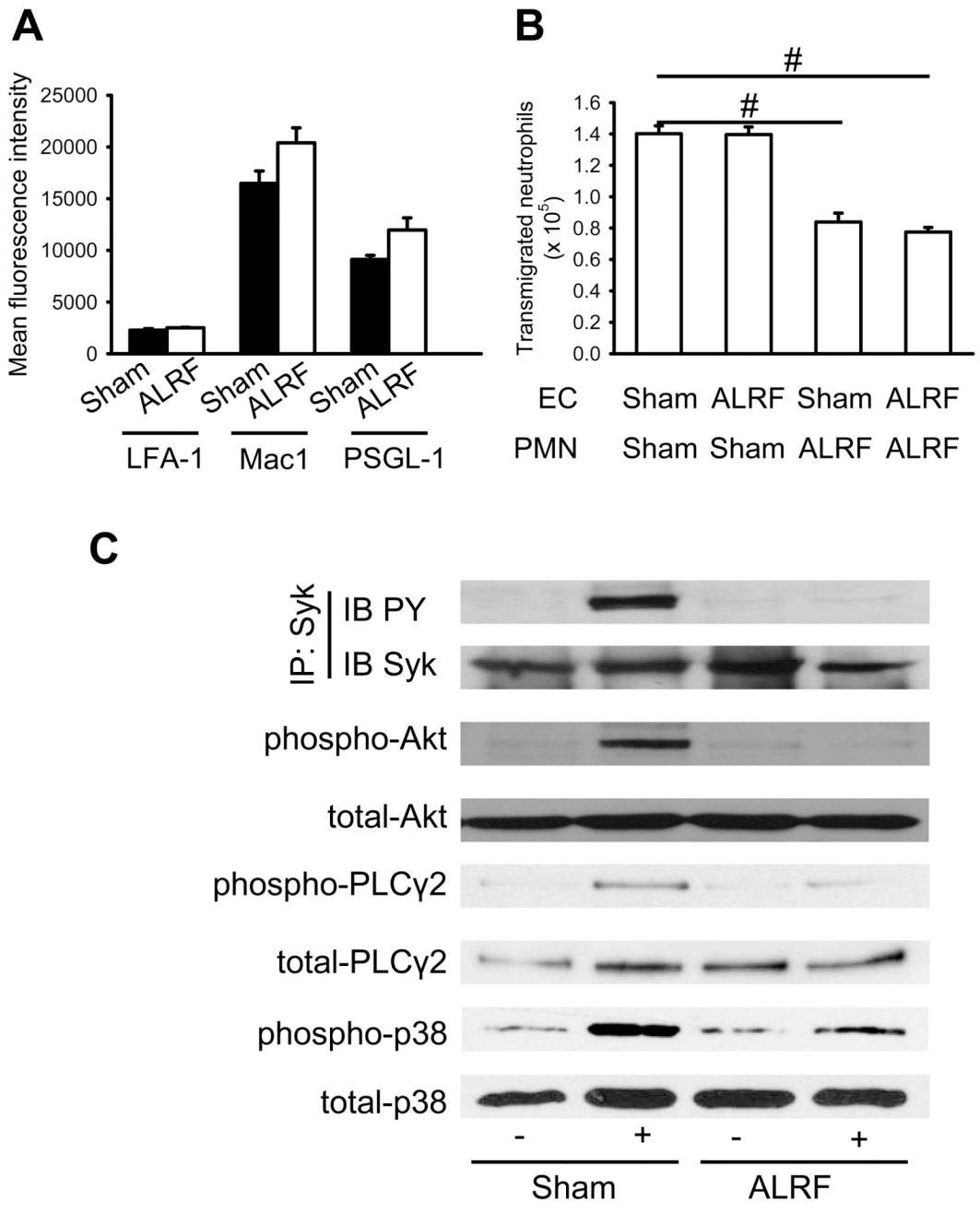

Figure 6. ALRF causes altered intracellular signaling and reduces transmigration *in vitro*

(A) Murine neutrophils were isolated from whole blood samples obtained from mice with ALRF and sham operated control mice and FACS analysis was performed to quantify the surface expression of PSGL-1, LFA-1 and Mac-1 (n=3). (B) Isolated neutrophils from mice with ALRF and sham operated control mice were allowed to transmigrate through bEnd.5 endothelial cells grown to confluence on a transwell filter *in vitro*. The endothelial cell layer was pretreated with plasma obtained from mice with ALRF or from sham operated control mice and the number of transmigrated neutrophils was determined (n=3). (C) Bone marrow–derived neutrophils were plated on uncoated (unstimulated) or E-selectin–coated wells for 10 minutes, and then lysates were prepared. Lysates were immunoprecipitated with anti-

Syk, followed by immunoblotting (IB) with a general phosphotyrosine (PY, 4G10) antibody. Lysates were immunoblotted with antibody to phosphorylated PLCγ2 (phospho PLCγ2 (Tyr1217)), total PLCγ2 (n = 3), phosphorylated Akt (n = 3), total Akt (n = 3), phosphorylated p38 MAPK (phospho-p38), or total p38 (*n* = 3). # $p < 0.05$.

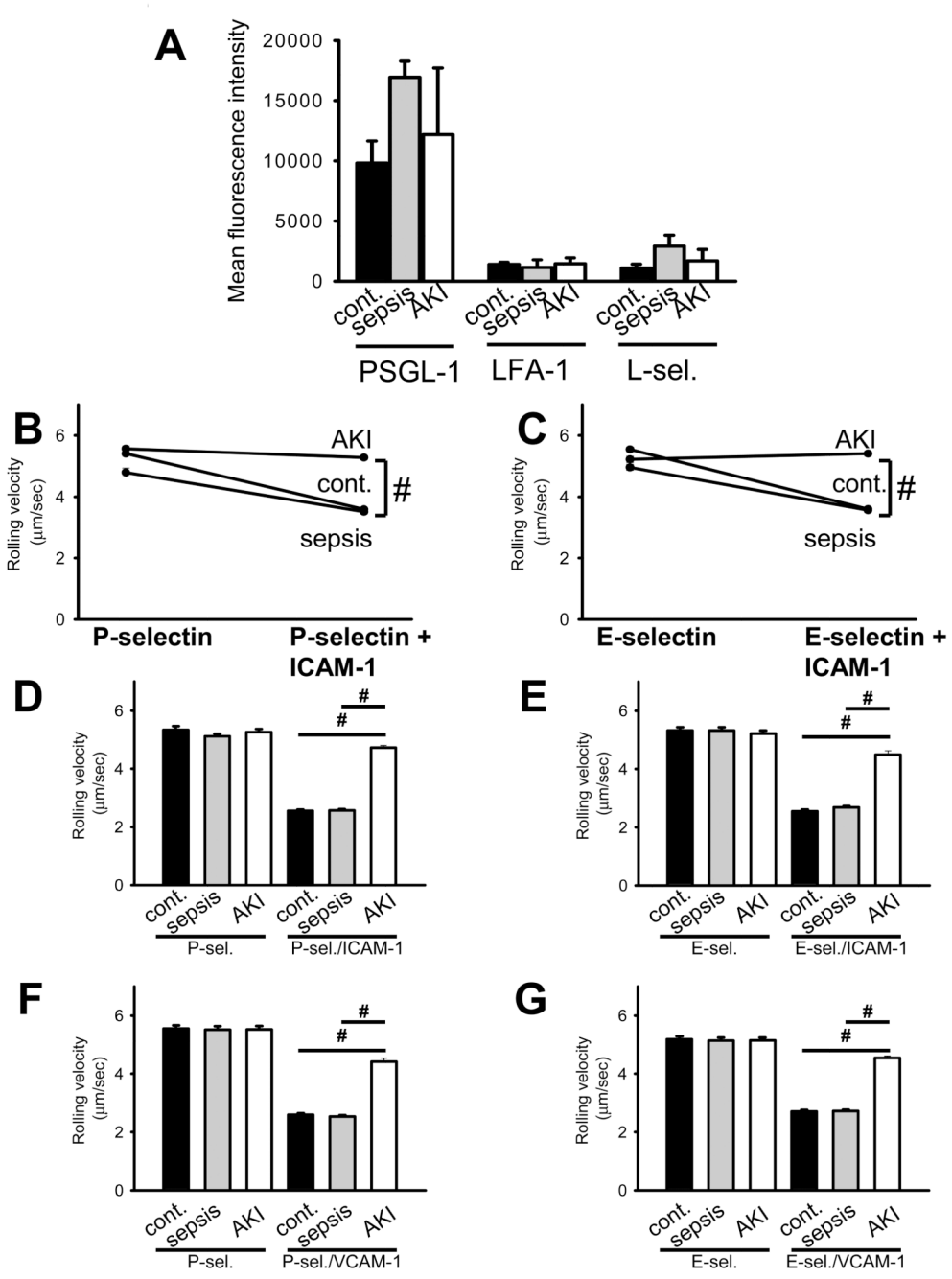

Figure 7. Selectin-mediated slow leukocyte rolling is abrogated in patients with sepsis-induced AKI

(A) Human neutrophils were isolated from whole blood samples obtained from patients presenting with sepsis or sepsis-induced AKI and healthy volunteers. FACS analysis was performed to quantify the surface expression of PSGL-1, LFA-1 and L-selectin on neutrophils (n=3–5). (B + C) The rolling velocity of neutrophils in whole blood samples from the three groups (healthy volunteers, sepsis, sepsis-induced AKI) was measured using microflow chambers coated with E-selectin or P-selectin alone and in combination with ICAM-1. (B) Average rolling velocity of neutrophils on P-selectin (left) and P-selectin/ICAM-1 (right) is presented as mean ± SEM (n=5). (C) Average rolling velocity of

neutrophils on E-selectin (left) and E-selectin/ICAM-1 (right) is presented as mean ± SEM (n=5). (D + E) Human neutrophils were isolated from whole blood samples obtained from healthy volunteers and preincubated with control serum and serum obtained from patients with sepsis or sepsis-induced AKI for 30 minutes. The rolling velocity of neutrophils was measured using microflow chambers coated with E-selectin or P-selectin alone and in combination with ICAM-1. (D) Average rolling velocity of neutrophils on P-selectin and P-selectin/ICAM-1 is presented as mean ± SEM (n=3). (E) Average rolling velocity of neutrophils on E-selectin and E-selectin/ICAM-1 is presented as mean ± SEM (n=3). (F + G) Human monocytes were isolated from whole blood samples obtained from healthy volunteers and preincubated with control serum and serum obtained from patients with sepsis or sepsis-induced AKI for 30 minutes. The rolling velocity of monocytes was measured using microflow chambers coated with P-selectin (F) or E-selectin (G) alone and in combination with VCAM-1. (F) Average rolling velocity of monocytes on P-selectin and P-selectin/VCAM-1 is presented as mean ± SEM (n=3). (G) Average rolling velocity of monocytes on E-selectin and E-selectin/VCAM-1 is presented as mean ± SEM (n=3). The wall shear stress in all flow chamber experiments was 5–6 dynes/cm^2. $^{\#}$ $p < 0.05$.

Table 1

Trauma					
	Venules	**WBC (x 10^6 cells x ml^{-1})**	**Diameter (μm)**	**Blood Velocity (μm/s)**	**Wall shear rate (1000 s^{-1})**
Sham	57	3.6 ± 0.8	27 ± 4	3.0 ± 0.3	1.8 ± 0.1
ALRF	55	3.9 ± 0.9	26 ± 4	2.9 ± 0.2	1.8 ± 0.2

LPS					
	Venules	**WBC (x 10^6 cells x ml^{-1})**	**Diameter (μm)**	**Blood Velocity (μm/s)**	**Wall shear rate (1000 s^{-1})**
Sham	34	2.5 ± 0.2	32 ± 1	2.5 ± 0.1	1.4 ± 0.1
ALRF	35	3.2 ± 0.4	30 ± 1	2.5 ± 0.1	1.5 ± 0.1

Table 2

	Sepsis	Sepsis + ALRF	p-value
Age [yrs]	43 ± 8.9	61.2 ± 7.4	n.s.
Weight [kg]	78.8 ± 7.1	88 ± 4.5	n.s.
Serumg creatinine level [mg/dl]	0.9 ± 0.1	2.5 ± 0.45	0.009
Serum urea nitrogen level [mg/dl]	25.6 ± 5.2	63.6 ± 10.8	0.013
Diuresis [ml/24h]	2136 ± 540	1184 ± 374	n.s.
APACHE II score	36 ± 3.4	33 ± 4.3	n.s.
SAPS score	45.5 ± 9.6	57.25 ± 8.2	n.s.
SOFA score	7.4 ± 1.4	9.8 ± 1.4	n.s.